

The developed method of analysis was intended to capture the most essential characteristics involved in the spiling reinforcement system in soft-ground tunneling without resorting to three-dimensional grids. However, the validity of the developed method of analysis remains to be tested. Further research should be done in areas such as field instrumentation and monitoring of prototype systems or large-scale centrifuge model testing. In this way the validity and effectiveness of the developed analytic methods can be checked and extended.

ACKNOWLEDGMENTS

The work presented in this paper is based on research supported by the U.S. Department of Transportation under contract No. DTRS-5681-C-00024. The author is extremely grateful for this support.

REFERENCES

1. G.E. Korbin and T.L. Brekke. Field Study of Tunnel Prereinforcement. *Journal of Geotechnical Engineering Division, ASCE*, Vol. 104, No. GT8, 1978.
2. K.M. Romstad, L.R. Herrmann, and C.K. Shen. Integrated Study of Reinforced Earth-I: Theoretical Formulation. *Journal of Geotechnical Engineering Division, ASCE*, Vol. 102, No. GT5, 1976.
3. J.M. Duncan and K.S. Wong. Hyperbolic Stress-Strain Parameters for Non-Linear Finite Element Analysis of Stress and Movements in Soil Masses. University of California, Berkeley, Rept. TE-74-3, 1970.
4. E.J. Cording and W.H. Hansmire. Displacements Around Soft Ground Tunnels. 5th Panamerican Congress on SM & FE, Session IV, General Rept., Buenos Aires, Nov. 1975.
5. G.E. Korbin and T.L. Brekke. Model Study of Tunnel Prereinforcement. *Journal of Geotechnical Engineering Division, ASCE*, Vol. 102, No. GT9, 1976.
6. J.B. Burland and C.P. Wroth. Settlement of Buildings and Associated Damage. Proc., Conference on Settlement of Structures, 1975.
7. R. Grant, J.T. Christian, and E.H. Vanmarcke. Differential Settlement of Buildings. *Journal of Geotechnical Engineering Division, ASCE*, Vol. 100, No. GT9, 1974.
8. J. Kreisel. Fifteenth Ranken Lecture: Old Structure in Relation to Soil Conditions. *Geotechnique*, Vol. 25, No. 3, 1975.
9. D.E. Polshin and R.A. Tokar. Maximum Allowable Non-Uniform Settlement of Structures. Proc., 4th International Conference on SM & FE, Vol. 1, 1957.
10. A.W. Skempton and D.H. MacDonald. Allowable Settlement of Buildings. Proc., Institution of Civil Engineers, Part 3, Vol. 5, 1956.
11. L. Bjerrum. Discussion. Proc., European Conference on Soil Mechanics and Foundation Engineering, Vol. II, Wiesbaden, 1963.
12. T.D. O'Rourke, E.J. Cording, and M. Boscardin. The Ground Movements Related to Braced Excavation and Their Influence on Adjacent Buildings. U.S. Department of Transportation, Rept. DOT-TST-76T-23, Aug. 1976.

Publication of this paper sponsored by Committee Subsurface Soil-Structure Interaction.

Compactive Prestress Effects in Clays

ALBERT DiBERNARDO AND C.W. LOVELL

The load-deformation behavior of natural clays is strongly influenced by the geologic maximum past pressure. If such clays are excavated and manipulated before compaction, the geologic effect is largely lost. However, the compaction process establishes a new prestress value, and the ratio of this prestress to the effective normal stress in a compacted fill forms a new overconsolidation ratio (OCR). If the material and compactive prestress values are held constant in a moderately high embankment, the OCR values range from quite high at lesser depths to unity in lower embankment locations. Consequently, the nature of the shearing and compressibility responses varies considerably with position in the embankment. Laboratory studies have been conducted on both compacted shales and clays to demonstrate the empirical prediction of the prestress value and its relative effect on saturated compressibility and undrained shear behavior. The prestress varies with the nominal compaction pressure and its rate of application, as well as with the material and its water content. This value is predicted from the conventional oedometer test on the as-compacted material. When the compacted materials are soaked at a variety of confining pressures, which simulate differing embankment positions, the volume changes are highly dependent on the major compaction variables and the prestress. To achieve a homogeneous and predictable load-deformation response in major embankments, it is necessary to better understand and control the prestress effected by compaction. The research discussed here was conducted to examine the compressibility behavior of a laboratory-compacted soil in the as-compacted and soaked condition. A highly plastic residual clay and a kneading type of com-

action were used. To determine the as-compacted compressibility characteristics, the compacted samples were trimmed to appropriate size and incrementally loaded in the oedometer. Of particular interest was the value of compactive prestress.

Early hypotheses concerning compaction of fine-grained soils explained the compaction process in terms of a predominant influence of individual clay particles (or clusters). More recently, the role of agglomerations or peds of clay particles has been emphasized.

BACKGROUND

Compaction Hypotheses

Barden and Sides (1) attempted to relate the engineering behavior of compacted clay to its fabric. Photomicrographs of the fabric of two clays revealed that the main difference between samples compacted

at different moisture contents was at the larger size levels. Observations revealed an apparently homogeneous fabric wet of optimum and 3-mm to 6-mm diameter pelletlike macropeds dry of optimum. These findings led to the following general analysis of the compaction process.

"At low compaction moisture contents the low dry density is caused by the presence of large air-filled macropores" (1, p. 1195). In addition, the macropeds, or clusters of clay particles, are able to resist the compaction pressure without much distortion. As the water content is increased, the macropores become filled with soil (easy slippage); the result is an increase in density. As the water content is increased further, the water layers increase in thickness, and the aggregates, easily distorted, fuse together making them indistinguishable. This, in turn, decreases compacted density (1).

Hodek (2) explained the characteristics and engineering behavior of a compacted soil in terms of a deformable aggregate model. He concluded that this model is appropriate to use in interpreting swell and compaction characteristics of a laboratory static compacted kaolinite. His theory of the compaction process is similar to that of Barden and Sides.

According to Garcia-Bengochea (3), pore-size distribution measurements for compacted clays have also provided strong evidence for a deformable aggregate model. He cites Bhasin (4) who found that as the compactive effort increases, the fraction of pores on the dry side of optimum decreases, whereas, on the wet side, the distribution remains the same. These findings are of interest because they directly affect compacted clay permeability, which, in turn, directly affects the rate of compressibility of compacted clay.

Hodek and Lovell (5) have proposed a model that explains the achievement of compacted unit weight for the laboratory static compaction of kaolinite. They propose that the initial soil fabric of the as-molded soil (before compaction) is that of aggregations of different size and water content. The size and distribution of these aggregates play an important role in the compaction process; that is, densification is associated with the decrease in interaggregate void ratio due to translation and rotation, the deformation of aggregates into the shape of available voids, and the reduction of intra-aggregate voids. Accordingly, the type of compaction and the aggregate-size distribution establish the fluid and continuity condition within the mass, and, once the air voids are no longer interconnected, little densification occurs regardless of the input effort. Hodek and Lovell (5) also introduce the concept of net energy imparted to the soil during the compaction process. It was found that the net energy required to obtain different conditions on the same moisture-density curve is inversely proportional to the aggregate size; uncomplicated mathematical models were developed to show this relationship.

Compressibility Characteristics

During the compaction process, the soil experiences the load for only a short time. The energy supplied in this short period is received by the soil skeleton, as an intergranular stress, and the pore fluids, as a pressure in each of the phases. Upon completion of the process, there is an induced prestress in the soil; this prestress may or may not be equal to the compaction pressure. According to Abeysekera (6), it is this value of compactive prestress that is important with respect to compacted clay behavior.

Woodsum (7) defined compactive prestress as analogous to the preconsolidation pressure of a natural soil; specifically, the apparent pressure effect caused by the compaction process. Lambe (8) similarly defined compactive prestress but realized that its value was affected by other factors, namely, time and chemical changes. For the purposes of this study, the compactive prestress will be defined as the precompression pressure, in terms of total stress, that has been induced in the soil as a result of the compaction process and is determined on an as-compacted oedometer specimen directly after compaction.

To determine compactive prestress Woodsum (7) statically compacted Fort Union clay and Mississippi loess directly in oedometer rings, allowed the soil to come to equilibrium with water under an applied load, and performed the conventional oedometer test. The data showed that as the confining pressure (P_0) remained constant and, as the compaction pressure (P_c) increased or the initial void ratio (e_0) decreased, the value of prestress increased. Moreover, the data suggest that although the value of prestress increased with increasing compaction pressure, the prestress ratio (P_p/P_c), which is similar to the overconsolidation ratio for saturated soils, varied slightly not increasingly as might be expected. This may mean that, for a given compaction process and type of soil, the efficiency of the process does not increase with increasing effort.

Abeysekera (6) determined the prestress induced by the kneading compaction of a shale material. The material was compacted at pressures ranging from 345 kN/m² to 1380 kN/m² (50 to 200 psi) and loaded in the as-compacted condition, either incrementally in the oedometer or at constant rate of strain. The elapsed time for each oedometer load increment was 10 minutes--the same loading time used by Yoshimi and Osterbert (9). The estimated prestress was determined in terms of total stress from the void ratio-log pressure curve using the Casagrande construction.

In the seven tests performed, Abeysekera (6) found the prestress values and the prestress ratio to range from 345 kN/m² to 865 kN/m² (50 to 126 psi) and 0.49 to 1.0, respectively. The ratio range is greater than Woodsum's (0.1 to 0.2). The difference in ratio range may be attributable to the differences between kneading and static methods, shale and clay, unsoaked condition and soaked condition, either singly or in combination. However, some interesting correlations can be made with Abeysekera's results.

Table 1 summarizes the results of other investigators who were concerned with the compressibility of compacted materials but not specifically with compactive prestress. If only the data related to soils are examined, it can be seen that static compaction methods are the most efficient with respect to induced prestress. Seed, Mitchell, and Chan (10) examined the effect of the difference in compaction method on the undrained shear strength of compacted clay; they found that static compaction resulted in smaller shear strains, lower pore water pressures, and higher strength values at low strains and that kneading compaction resulted in larger shear strains, higher pore water pressures, and lower strength at low strains. This appears to be a reasonable explanation of differences in statically induced prestress and prestress induced by kneading methods.

EXPERIMENTAL APPARATUS AND PROCEDURE

The soil used in this study was obtained from Perry County, Indiana. It will hereafter be referred to

Table 1. Compaction pressure and prestress (6).

Investigator	Material	Compaction Mode	Compaction Pressure [P _c (psi)]	Dwell Time (sec)	Prestress Values [P _s (psi)]	Prestress Ratio (P _s /P _c)
Cambell (1952)	Bituminous concrete	Static	2,500	60	150-210	0.06-0.08
Yoshimi and Osterberg (1963)	Silty clay	Static (20 psi/min)	94	280	94	1.00
Mishu (1963)	Residual clay	Kneading (30 blow/min)	95	1	36.1	0.38
			125	1	36.1	0.29
			170	1	55.6	0.33
Abeyesekera (1978)	Shale aggregate	Kneading (30 blow/min)	50	1	50	1.00
			100	1	68-74	0.68-0.74
			200	1	98-126	0.49-0.63

as St. Croix clay. The St. Croix clay is medium gray-brown at its natural moisture content. It is classified as a fat clay (CH) and falls within the AASHTO classification of an A-7-6 material.

The kneading method of compaction was selected for use in this study for two reasons: (a) The compaction characteristics obtained are comparable, for the same soil, to those obtained by sheepfoot- and pneumatic-type rollers on actual earthen embankments, and (b) the degree of uniformity with respect to moisture content and density is greater than that of other methods.

The soil was compacted in 5 approximately equal layers at a rate of 30 tamps per minute per layer. Between layers, the top surface was scarified to ensure compacted mass homogeneity. A constant compaction pressure was maintained throughout the process; the value was based on moisture-density relations for the impact method. The results and implications of this procedure will be discussed later.

Typically, density and water content are the prescribed elements in an end-result approach and are based on results obtained by the laboratory impact method. It was therefore considered appropriate to use the impact moisture-density relations as a base reference for the kneading method.

The moisture-density curves for the three basic impact energy levels used are shown in Figure 1. Each energy level is characterized as follows.

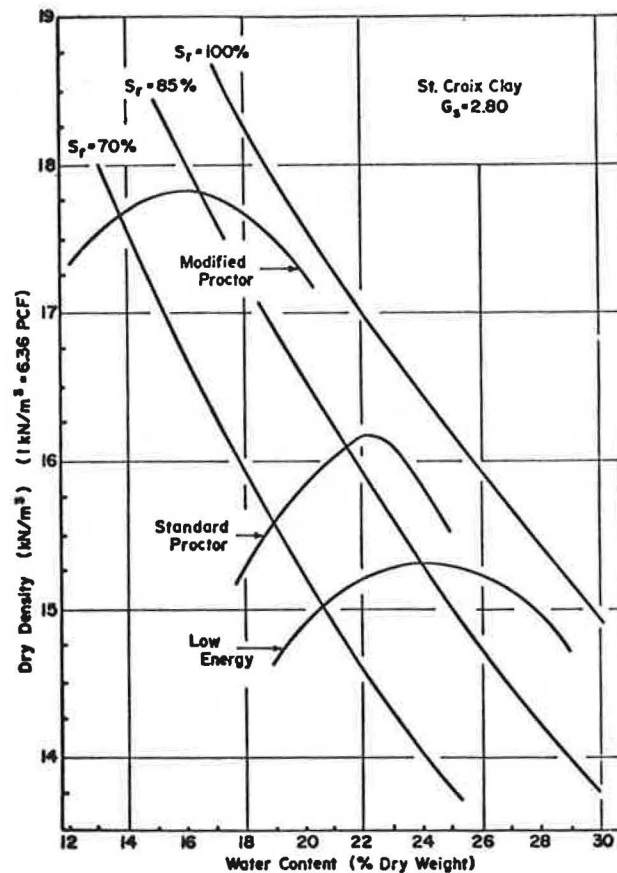
1. Low-energy Proctor--304.8 mm (12 in.) drop, 24.5N (5.5 lb) rammer, 3 layers, 15 blows per layer.
2. Standard Proctor--304.8 mm drop, 24.5N rammer, 3 layers, 25 blows per layer.
3. Modified Proctor--457.2 mm (18 in.) drop, 44.5N (10 lb) rammer, 3 layers, 25 blows per layer.

The compaction assembly and procedure were as specified in AASHTO T99070; however, fresh samples were used for each point on the curve.

A series of kneading compaction tests was performed on the St. Croix clay using different compaction pressures. For each pressure a moisture-density relation was obtained for a range of moisture contents between 4 percent wet and dry of optimum. These relations were correlated approximately to the three impact levels to select a kneading compaction pressure that would produce the same densities at equivalent water contents.

A fixed-ring consolidation cell was used in this study; it will be referred to as an "oedometer" in subsequent discussions. The oedometer ring was 63.5 mm (2.50 in.) in diameter, 2.54 mm (1 in.) in height, and 19.1 mm (0.75 in.) in wall thickness. Following a seating load adjustment period (typically 10 min), the applied pressure on the compacted sample was increased, using a load increment ratio (LIR) of 0.5 to 15.2, 22.6, 34.0, 49.5, 76.5 kN/m², and so on until the prestress value for the partic-

Figure 1. Moisture-density-energy relations for impact method (11).



ular sample could be well defined. The duration of each load was 10 minutes; dial readings were typically recorded at 0, 0.1, 0.5, 1, 2, 4, 8, and 10 minutes.

The 10-minute load duration criterion was based principally on the findings of Yoshimi (12). To determine what load increment ratio to use for the as-compacted compression test, it was decided that the following requirements should be met.

1. A large portion of the compression must take place within 10 minutes.
2. As few loads as possible should be used, to limit moisture loss by evaporation.
3. The prestress value should be accurately defined using the Casagrande construction.

If an LIR = 1 were used, the first and second requirements would be satisfied; however, the third requirement might not be, based on the results of

Leonards and Girault (13) for determining the pre-consolidation value for saturated soils. If an LIR = 0.1 or 0.2 were used, the third requirement would be satisfied, but the first and second requirements would not be (12). Ideally, a load increment ratio equal to actual field loading conditions should be used; however, this ratio is dependent on a given application and may be difficult to determine. An LIR = 0.5 was chosen because it most suitably matched the requirements.

RESULTS

As-Compacted Compressibility

The compaction variables used to characterize each as-compacted compressibility test sample are defined as follows.

1. Water content ($w, \%$)--the average of the as-compacted moisture determinations.
2. Dry density ($\gamma_d, \text{kN/m}^3$)--the dry density of the oedometer sample computed from its unit weight, water content (w), and volume.
3. Compaction pressure ($P_c, \text{kN/m}^2$)--the maximum dynamic kneading foot pressure applied during compaction, expressed nominally.

The other computed variables were initial degree of saturation ($S_r, \%$) and initial void ratio (e_o). Both were calculated from the first and second variables just defined.

The compaction water contents ranged between 4 percent wet and dry of optimum and were based on the results of the impact method. Thirty-two as-compacted compressibility tests were performed; the values of the previously defined compaction variables are listed in Table 2. In this table and in subsequent discussions the sample number characters are defined as follows: L, S, M represent the com-

Table 2. Initial compaction variables for as-compacted compressibility samples (11).

Sample No.	Water Content (%)	Dry Density γ_d (kN/m^3)	Compaction Pressure P_c (kN/m^2)	Degree of Saturation S_r (%)	Initial Void Ratio e_o
LD1	20.60	13.97	460	59.77	0.9649
LD2	20.60	14.85	525	65.26	0.8838
LD3	20.51	14.27	426	62.15	0.9240
LO1	23.26	15.74	426	80.14	0.8126
LO2	23.85	15.77	558	89.62	0.7451
LO3	24.27	14.91	683	80.68	0.8423
LW2	27.94	14.88	525	92.47	0.8460
LW3	26.98	14.82	657	88.42	0.8544
SD4	18.95	15.26	788	66.40	0.7990
SD8	19.38	14.62	788	61.82	0.8770
SD9	19.59	15.06	788	66.58	0.8238
SD10	19.37	15.65	788	71.87	0.7545
SO3	12.37	15.76	657	80.61	0.7423
SO8	21.71	15.78	657	82.02	0.7411
SO9	21.21	15.99	657	82.70	0.7180
SO11	21.65	15.72	814	81.12	0.7473
SO12	22.32	16.15	788	89.20	0.7066
SO13	22.67	16.25	762	92.92	0.6905
SO16	22.68	15.97	762	88.18	0.7202
SW2	25.38	15.24	722	88.67	0.8014
SW3	25.71	15.13	722	88.27	0.8155
SW4	25.05	15.42	722	89.80	0.7810
SW6	24.72	15.64	722	91.49	0.7565
SW7	24.87	15.38	722	88.66	0.7854
SW8	24.71	15.68	722	92.08	0.7514
MD1	14.67	18.31	3191	82.10	0.5003
MD2	13.96	17.65	3071	70.23	0.5565
MO1	16.20	17.97	2905	85.90	0.5281
MO2	15.71	18.10	2735	85.10	0.5168
MW1	19.59	16.99	2466	87.85	0.6243
MW3	19.74	16.87	2439	88.05	0.6277
MW5	19.57	16.86	2466	87.18	0.6285

paction condition corresponding to the equivalent low-energy, standard Proctor, and modified Proctor impact levels, respectively. D, O, or W represent dry, at, or wet-of-optimum conditions, respectively; and 1, 2, ..., and so forth represent the sample number for that condition. For example, the sample designated MD1 is the first sample compacted to a dry of optimum condition using an equivalent modified Proctor kneading compaction pressure.

Figure 2 shows the effects of increasing water content and degree of saturation on compressibility behavior for samples compacted to equivalent standard Proctor conditions. As may be inferred, there is a marked difference in the compressibility behavior for wet- and dry-side samples depending on the range of consolidation pressure considered. That is, in the low-pressure range, the wet-side sample is more compressible than the dry-side sample, whereas in the high range the opposite is true.

Lambe (8,14) explained this behavior in terms of compacted clay structure, colloidal chemistry, and soil-particle rearrangement. However, more recently, Hodek and Lovell (15) examined this behavior in terms of pore-size distribution, pore-size magnitude, and deformable aggregate theory. Based on supporting evidence (2,3,16), their explanation can be stated as follows.

1. Dry-side compressibility--the pores are typically large and numerous; the clay aggregates are shrunken, hard, and brittle; compressibility is governed by the collapse of large pores under straining.

2. Wet-side compressibility--the pores are small and numerous; the clay aggregates are swollen and plastic; compressibility is governed by the fusing of aggregates under load.

In view of this explanation, a dry-side sample would compress less in the low-pressure range due to the large intergranular forces resulting from the many well-developed menisci. However, on loading, these forces are overcome, and the brittle aggregates displace into adjacent pores. Consequently, a large amount of compression occurs because of the large amount of available interaggregate pore space. On the other hand, a wet-side sample compresses more in the low-pressure range because of the smaller number of developed menisci (high degree of saturation) and less in the higher range because of the relatively small number of large interaggregate pores.

Figure 3 shows the effect of increasing compaction pressure on the compressibility behavior of samples compacted near optimum. The slope of the curves within the respective high-pressure ranges becomes steeper (i.e., increasingly more negative) with decreasing compaction pressure. With respect to the structural models previously discussed, this suggests that for dry-side samples the magnitude and frequency of the large pore mode decreases with increasing compaction pressure.

Compactive Prestress

The results presented in the previous section illustrate compressibility behavior within specific ranges of applied pressure. However, an important characteristic not considered is the value of compactive prestress. Clearly, its value could be useful in design, because the compressibility behavior of the mass may be different at embankment confining pressures above and below this value. That is, each specific value of compactive prestress, as determined in the manner presented in this section, is the approximate pressure value

Figure 2. Effect of moisture content on compressibility (standard Proctor) (11).

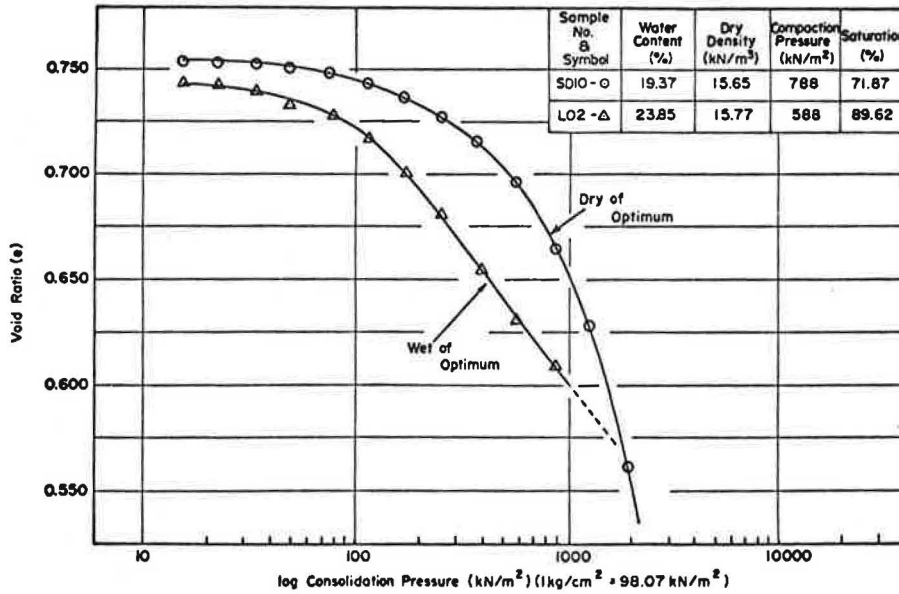
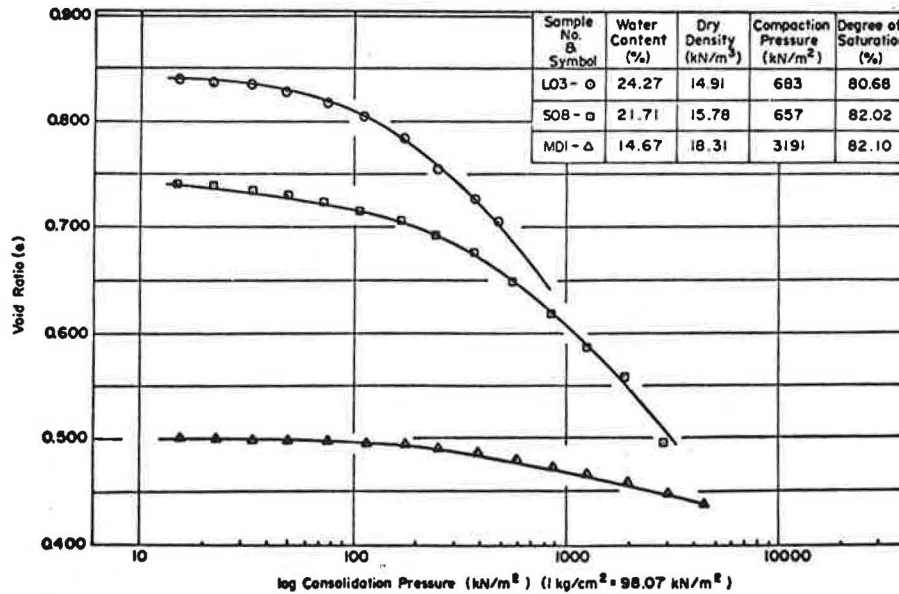


Figure 3. Effect of compactive effort on compressibility (near optimum) (11).



below and above which low-range compressibility behavior and high-range compressibility behavior, respectively, occur.

The value of compactive prestress (P_s) and the prestress ratio (P_s/P_c) for each of the thirty-two as-compacted compressibility test samples are listed in Table 3. Each value of compactive prestress was determined from its corresponding e -log p curve using the Casagrande approximation commonly employed for determining the most probable preconsolidation pressure for saturated soils. In the strictest sense, its use may be unjustified. However, the current state of the art is such that little is known of the fundamental relationships governing unsaturated compression.

Figure 4 shows the values of compactive prestress plotted at their respective values of water content, dry density, and equivalent impact effort level. The 87 percent saturation curve was arbitrarily

selected and plotted in this figure and, for the purpose of this discussion, will be referred to as a means of separating wet and dry compaction conditions.

From Figure 4, the following general conclusions may be drawn with respect to prestressing capacity.

1. For dry of optimum conditions ($S_r < 87\%$):
 - (a) At a given equivalent impact effort level, as the water content increases, the value of compactive prestress decreases.
 - (b) As the equivalent impact effort increases, the value of compactive prestress also increases.
2. For wet of optimum conditions ($S_r > 87\%$):
 - (a) At a given equivalent impact effort level, the capacity for prestressing is small and remains virtually unchanged with increasing water content.
 - (b) As the equivalent impact effort level increases, the capacity for prestressing is virtually unchanged.

Table 3. Values of compactive prestress and prestress ratio (11).

Sample No.	Compactive Prestress [P _s (kN/m ²)]	Compaction Pressure [P _c (kN/m ²)]	Prestress Ratio (P _s /P _c)	Degree of Saturation [S _r (%)] ^a
LD1	290	460	0.63	59.8
LD2	315	525	0.60	65.3
LD3	220	426	0.52	62.2
LO1	185	426	0.43	80.1
LO2	155	588	0.26	89.6
LO3	85	683	0.12	80.7
LW2	76	525	0.14	92.5
LW3	72	657	0.11	88.4
SD4	505	788	0.64	66.4
SD8	470	788	0.60	61.8
SD9	490	788	0.62	66.6
SD10	500	788	0.63	71.9
SO3	410	657	0.62	80.6
SO8	340	657	0.52	82.0
SO9	235	657	0.36	82.7
SO11	105	814	0.13	81.1
SO12	95	788	0.12	89.2
SO13	105	762	0.14	92.9
SO16	125	762	0.16	88.2
SW2	95	722	0.13	88.7
SW3	135	722	0.19	88.3
SW4	80	722	0.11	89.8
SW6	160	722	0.22	91.5
SW7	90	722	0.12	88.7
SW8	55	722	0.08	92.1
MD1	830	3191	0.26	82.1
MD2	1120	3071	0.36	70.2
MO1	1030	2905	0.35	85.9
MO2	1100	2753	0.40	85.1
MW1	85	2466	0.03	87.9
MW3	86	2439	0.04	88.1
MW5	150	2466	0.01	87.2

^aThe degrees of saturation were rounded to the nearest tenth.

This suggests that at dry-side water contents, prestressing capacity is largely affected by compaction water content and compaction pressure. In addition, compactive prestress is little affected by water content and compaction pressure for initially wet samples. Finally, for the range of saturation considered in this study, the prestress ratio is always less than one, which may indicate that not all of the energy delivered is achieving densification.

In this connection, it is important to realize that the compaction pressures reported here are only nominal pressures; that is, they are the pressures expended by the kneading compactor during the compaction process. Therefore, the actual prestress ratios (i.e., compactive prestress/effective compaction pressure) are more than likely greater than the values presented here.

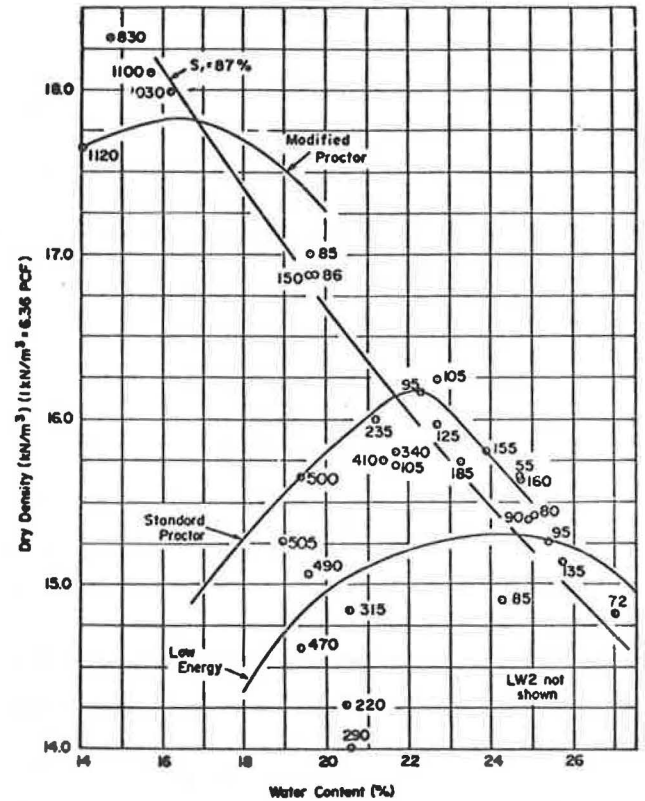
Statistical Correlations

The predictive models presented here were developed using the Statistical Package for the Social Sciences (SPSS) procedural programs on Purdue University software. It should be mentioned that any best model isolated by these programs is highly dependent on the procedure used, and an equivalent model may not be established given another set of procedures.

The first phase of the isolation process involved plotting the independent variables against the dependent variable. This was facilitated using the SPSS procedure SCATTERGRAM. If the scatter plots showed a linear relationship, the independent variable was considered highly correlated with the dependent variable. If a linear trend was not found, the independent variable was considered statistically insignificant.

The next step was to isolate a subset of the

Figure 4. Prestress values (kN/m²) for as-compacted compressibility tests (11).



independent variables considered highly correlated with the dependent variable, so that an optimal expression with as few variables as possible could be established. This was achieved using the automatic SPSS search procedure STEPWISE. This procedure combines a forward inclusion of independent variables already in the model at each successive step. In addition, it conducts a statistical test to screen out any independent variable that is too highly correlated with the independent variables already in the model.

The final step of the isolation process was to obtain the best estimated prediction model from the subset of independent variables isolated by the STEPWISE procedure. This was done using the SPSS procedure REGRESSION [developed by Nie, et al. (17)]. Various regression equations were obtained using different combinations. From these, the procedure for selecting the best model was based on the following statistical criteria.

1. For the overall multiple regression equation, (a) The coefficient of multiple determination (R²) is greater than 0.65; that is, at least 65 percent of the variation must be explained by the variables included in the model. (b) The adjusted coefficient of multiple determination (R²_a) must increase with each additional independent variable entered in the model. (c) The overall F-test at the α = 0.05 significance level must be met. (This tests for multiple linearity of the model.)

2. For the partial regression coefficients, (a) The F-test for each partial regression coefficient at the α = 0.05 significance level must be met. (This tests whether an independent variable should be dropped from the model.) (b) The coefficients of partial determination (r_{i,jk}) are significant. (c) The 95 percent confidence limit for each b_i is

small and does not cross zero. [This restriction is similar to (a).]

3. For the computed residuals, (a) The scatter plots of the residuals versus the independent variable(s) show normal constancy of variance trends. (b) The residuals are normally distributed random variables; that is, the values of e_k/MSE (residuals divided by the error root mean square) must range between ± 3 .

When all criteria were suitably met by more than one model, the model with the fewest variables was selected, provided there was no appreciable difference (i.e., less than 5 percent) in either of the R^2 or R^2_a values.

Based on the foregoing, the following prediction model was selected for compactive prestress (P_s).

$$P_s = -343.13 - 0.0020w^2 \cdot P_c + 48.91 P_c^{1/2}$$

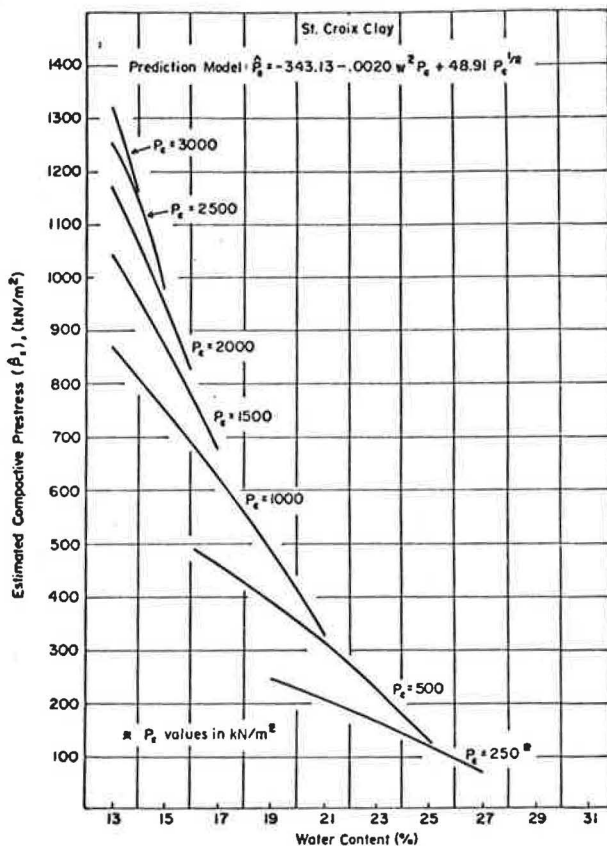
where

- P_s = estimated value of compactive prestress in kN/m^2 ,
- $w^2 \cdot P_c$ = interaction term between water content (%) squared and compaction pressure (kN/m^2), and
- $P_c^{1/2}$ = the square root of compaction pressure (kN/m^2)^{1/2}.

The R^2 value was 88 percent. In addition, all of the other statistical criteria were suitably met. A graphic representation of this relationship is presented in Figure 5.

As shown in this figure, for a given water content the estimated compactive prestress increases with increasing compaction pressure. Woodsum (7)

Figure 5. Prediction of compactive prestress (11).



and Abeyesekera (6) obtained similar results. Also, for a given compaction pressure an increase in water content is accompanied by a decrease in compactive prestress. More clearly, at a given effort level, an increase in water content reduces prestressing capacity.

The relations shown in Figure 5 are not entirely applicable for the values of water content and compaction pressure plotted. Rather, they are applicable only for a joint region of observations; that is, the region covered by both independent variables (18). Neither model can be used with confidence in design until the results presented here are correlated with results for field-compacted samples of the same soil. Such research is currently in progress at Purdue University.

CONCLUSIONS

The experimental and statistical results of this study lead to the following conclusions.

1. For an increasing water content and equivalent impact level, the as-compacted compressibility behavior was in agreement with the results presented by Wilson (19), Lambe (8), and Wahls et al. (20). It is believed that this behavior can be explained in view of more recent evidence (1,5,15) concerning compacted clay macrostructure.
2. Dry of optimum, the value of compactive prestress decreased with increasing water content and increased with increasing equivalent impact effort level. Wet of optimum, the value of compactive prestress was not influenced appreciably by varying the initial compaction variables.
3. For the range of partial saturation considered, the ratio of compactive prestress to nominal compaction pressure was less than unity. This ratio tended to decrease with increasing initial degree of saturation.
4. The best predictive model for compactive prestress was isolated using the SPSS procedures SCATTERGRAM, STEPWISE, and REGRESSION. The proposed model was statistically valid and accurate.

ACKNOWLEDGMENT

The authors are grateful to the Indiana State Highway Commission and the Federal Highway Administration for the financial sponsorship of this study. The research was administered through the Joint Highway Research Project, Purdue University, West Lafayette, Indiana.

The contents of this paper reflect the view of the authors who are responsible for the facts and the accuracy of the data presented.

REFERENCES

1. L. Barden and G.R. Sides. Engineering Behavior and Structure of Compacted Clay. Journal of the Soil Mechanics and Foundations Division, ASCE, Vol. 96, No. SM4, 1970, pp. 1171-1200.
2. R.J. Hodek. Mechanism for the Compaction and Response of Kaolinite. Purdue Univ., West Lafayette, Ind., Joint Highway Research Project, Rept. 72-36, Dec. 1972.
3. I. Garcia-Bengochea. The Relation Between Permeability and Pore Size Distribution of Compacted Clayey Silts. Purdue Univ., West Lafayette, Ind., Joint Highway Research Project, Rept. 78-4, May 1978.
4. R.N. Bhasin. Pore Size Distribution of Compacted Soils After Critical Region Drying.

- Purdue Univ., West Lafayette, Ind., Joint Highway Research Project, Rept. 75-3, May 1975.
5. R.J. Hodek and C.W. Lovell. Soil Aggregates and Their Control Over Soil Compaction and Swelling. TRB, Transportation Research Record 733, 1979, pp. 94-99.
 6. R.A. Abeysekera. Stress Deformation and Strength Characteristics of a Compacted Shale. Purdue Univ., West Lafayette, Ind., Joint Highway Research Project, Rept. 77-24, May 1978.
 7. H.C. Woodsum. The Compressibility of Two Compacted Clays. Master's thesis, Purdue Univ., West Lafayette, Ind., 1951.
 8. T.W. Lambe. The Engineering Behavior of Compacted Clay. Journal of the Soil Mechanics and Foundations Division, ASCE, Vol. 84, No. SM2, 1958, pp. 1-35.
 9. Y. Yoshima and J.D. Osterberg. Compression of Partially Saturated Cohesive Soils. Journal of the Soil Mechanics and Foundations Division, ASCE, Vol. 89, No. SM4, 1963, pp. 1-23.
 10. H.B. Seed, J.B. Mitchell, and C.K. Chan. The Strength of Compacted Cohesive Soils. Research Conference on Shear Strength of Cohesive Soils, Boulder, Colo., 1960, pp. 877-964.
 11. A. DiBernardo and C.W. Lovell. The Effect of Laboratory Compaction on the Compressibility of a Compacted Highly Plastic Clay. Purdue Univ., West Lafayette, Ind., Joint Highway Research Project, Rept. 79-3, Feb. 1979.
 12. Y. Yoshimi. One Dimensional Consolidation of Partially Saturated Soil. Ph.D. diss., Northwestern Univ., Evanston, Ill., 1958.
 13. G.A. Leonards and P. Girault. A Study of the One-Dimensional Consolidation Test. Proc., Fifth International Conference on Soil Mechanics and Foundation Engineering, Paris, Vol. 1, 1961, pp. 213-218.
 14. T.W. Lambe. The Structure of Compacted Clay. Journal of the Soil Mechanics and Foundations Division, ASCE, Vol. 84, No. SM2, 1958, pp. 1-34.
 15. R.J. Hodek and C.W. Lovell. A New Look at Compaction of Landfills. Presented at AEG Conference, Hershey, Pa., Oct. 18, 1979.
 16. M.A. Reed. Frost Heaving Rate of Silty Soils as a Function of Pore Size Distribution. Purdue Univ., West Lafayette, Ind., Joint Highway Research Project, Rept. 77-15, 1977.
 17. N.H. Nie, et al. Statistical Package for the Social Sciences. 2nd ed. McGraw-Hill, New York, 1975.
 18. J. Neter and W. Wasserman. Applied Linear Statistical Models. Irwin, Homewood, Ill., 1974.
 19. S.L. Wilson. Effect of Compaction on Soil Properties. Proc., Conference on Soil Stabilization, MIT, Cambridge, Mass., 1952, pp. 148-158.
 20. H.E. Wahls, C.P. Fisher, and L.J. Langfelder. The Compaction of Soils and Rock for Highway Purposes. FHWA-RD-73-8, 1966.

Publication of this paper sponsored by Committee on Earthwork Construction.